

RESEARCH ON CALCULATION OF SLOPE FAILURES CONSIDERING UNSTABLE TRANSIENT SURFACE DUE TO RAIN

Trung Quan NGUYEN¹, Huy Cong VU¹, Ly Trieu PHAM¹, Le Thuan NGUYEN², Van Huong NGUYEN^{1*}

¹The University of Danang - University of Science and Technology, Vietnam

²Central Rural Electric Project Management Board - Central Power Corporation, Vietnam

*Corresponding author: nvhuong@dut.udn.vn

(Received: September 08, 2024; Revised: September 21, 2024; Accepted: October 15, 2024)

DOI: 10.31130/ud-jst.2024.564E

Abstract - Slope landslides are one of the natural hazards that are gradually appearing more and more in number and intensity, causing serious damage to people, property, and infrastructure. Many studies have shown that climatic factors such as rainfall and human activities are important causes of landslides. The infiltration of rainfall changes the water content of the unsaturated zone (Vadose Zone), thereby causing instability. In this study, a 2-dimensional slope stability model was established using the seepage analysis module (SEEP/W) and stability (SLOPE/W), which considers the impact of rainfall changes, the existence of tree canopy and trunk, the soil reinforcement effect of tree roots, water absorption of tree roots, and the impact of tree roots on soil permeability, thereby calculating slope stability, applied to the Dak Pring hydropower plant project (Cha Val commune, Nam Giang district, Quang Nam province). The paper aims at a more comprehensive and detailed approach to seepage - slope stability calculation models than traditional solutions.

Key words - Slope erosion; unsaturated zone; rainfall; seepage; stability.

1. Introduction

Slope landslides are phenomena in which soil, rock, or other materials slide downward, reducing the stability of the slope, usually occurring in adverse situations or under the effects of human activities. This phenomenon can occur suddenly or gradually, depending on several factors such as topography, geology, earthquakes, erosion, seepage due to rainfall, vegetation, human activities, among others. Among these factors, rainfall is considered the most common cause of landslides, especially in tropical regions. This is because in tropical regions, rains are often prolonged, and in mountainous areas, the soil layer covering the bedrock has a relatively high-water absorption. Landslides often cause serious casualties, damage to infrastructure, loss of productive land, traffic congestion, environmental impacts, changes to natural landscapes, etc. Therefore, landslides are among the most damaging natural disasters in the world. Indeed, in 1999, heavy rains caused landslides in Vargas, Venezuela, resulting in 30,000 deaths and affecting millions [1]. Also, in 1999, a major landslide occurred following an earthquake in Izmit, Turkey, killing more than 17,000 people and causing extensive property damage [2]. In 2013, landslides under intensive rainfall happen in Uttarakhand, India, leaving more than 5,700 people missing and causing extensive damage to infrastructure [3]. In 2014, a landslide in Oso, Washington, USA, killed 43 people and destroyed many homes [4]. In 2015, after a

strong earthquake, many landslides occurred, affecting thousands of people and causing significant damage to infrastructure in Nepal [5]. In China, in 2017, a landslide in Sichuan killed at least 10 people and left many others missing [6]. Global estimates of economic losses due to landslides range from \$1 to \$10 billion per year [7]. Meanwhile, the total annual damage caused by landslides in Vietnam is estimated to be hundreds of billions of dongs [8]. Nepal is one of the most affected countries in the world, due to its mountainous terrain and complex climate. India, Indonesia, and China also face similar problems, with many areas prone to landslides due to their topography and weather conditions [9 - 12].

Vietnam is considered one of the most vulnerable countries in the Asia Pacific region to landslides. This is mainly due to its diverse topography with many mountainous and steep areas, along with its tropical monsoon climate conditions. Heavy and prolonged rainfall events during the rainy season, especially after tropical storms, often cause landslides, affecting people, transport infrastructure, and agricultural production. Furthermore, unsustainable natural resource exploitation and rapid urbanization also contribute to increased landslide risks [13], [14]. In 2021, a landslide occurred in Hoanh Bo district, Quang Ninh, killing two people and damaging many houses [15]. Also in Quang Ninh, in 2017, a landslide occurred in Tan Lac district, 5 deaths and causing serious property damage [16]. In 2018, in Moc Chau district, Son La, landslides caused many roads to be blocked, affecting traffic and people's lives [17]. In 2020, landslides after heavy rains killed 4 people and left many missing, causing great damage to agriculture in Nghe An [18]. In Tra Leng, Quang Nam, in 2020, there were 8 deaths and dozens of houses buried after a serious landslide [19]. In addition, a serious landslide occurred in Rao Trang, Thua Thien - Hue in 2020 as a result of prolonged heavy rain due to the influence of storm No. 7 and steep terrain characteristics.

In the context of increasing climate change, extreme weather events such as heavy rains are becoming more frequent, increasing the risk of landslides in many areas, especially mountainous areas. Therefore, studying landslides is not only a scientific requirement but also a practical task to protect human life and property, while ensuring a sustainable living environment. In this article, the authors focus on a solution to prevent slope landslides

applied to the Dak Pring hydropower plant (Quang Nam province), considering the influence of climatic factors over time (changes in rainfall, temperature, humidity, evaporation, and wind) and the connection between soil, rock, root layers, and vegetation.

2. Methodology

Up to now, there have been many studies conducted on the mechanism of seepage and slope failure due to rainfall. The approaches of these studies have been sorted into different groups of methods. (1) Physical model experiments [20 - 24]; (2) Physical model experiments with mathematical models [25]; (3) Physical model experiments in the laboratory to determine the physical properties of soil, combined with mathematical modeling and field surveys [26 - 28]. The results of the above studies have shown that volumetric water content (VWC) and pore water pressure (PWP) have spatial and temporal variations in slopes affected by wet and dry cycles. The failure mechanism of rainfall-induced landslides is mainly related to the development of an upper moisture layer, leading to increased pore water pressure (loss of suction or development of positive PWP) in the soil. The increase in PWP leads to a decrease in the shear strength of the soil, causing slope failure. The stability of the slope is directly affected by the changes in VWC and PWP, and these two parameters depend on the rainfall intensity, soil permeability coefficient, soil saturation, slope topography, and vegetation.

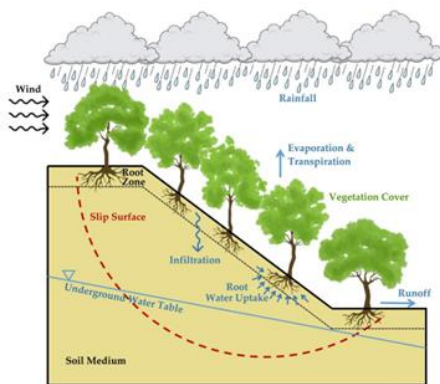


Figure 1. The hydrological cycle and the main consequences of rainfall on soil slopes [29]

In addition, vegetation cover on slopes also has a significant influence on slope stability. The impact of vegetation on slope stability takes two general forms: mechanical and/or hydrological. The mechanical impact is mainly related to the root system (depth, width, and texture); the roots anchored in the soil will support the above-ground biomass, creating a reinforced soil frame, helping to reduce the possibility of slope failure. In addition, root systems can also negatively impact slope stability by generating additional loads (due to roots and trunks), increasing moisture retention leading to increased pore water pressure, reducing soil strength, and weakening soil structure. Moreover, the weight of trees and wind affecting the equilibrium of the slope should also be considered. Figure 1 shows a diagram of the

conceptualization of the model and the processes influencing the slope stability assessment [29]. The hydrological impact of vegetation on slope stability relates to changes in soil moisture. Vegetation can reduce soil moisture by intercepting rainfall on the ground (due to some precipitation remaining on tree crowns and trunks) and by absorbing water from the soil through its roots. Conversely, vegetation also promotes water infiltration rather than surface runoff (holding water on the surface), which leads to increased soil moisture during and after rainfall events, potentially destabilizing slopes.

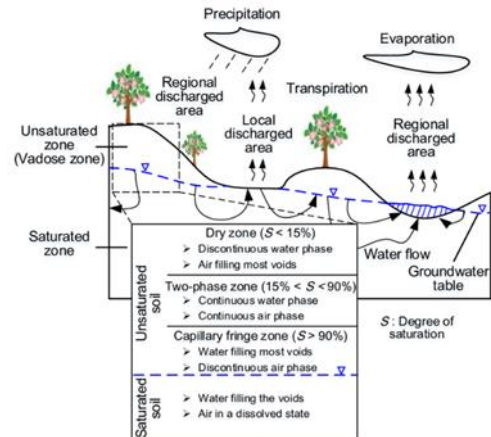


Figure 2. Subdivisions of Vadose zone (unsaturated zone) [30]

The Vadose Zone, also known as the unsaturated zone, is the part of the soil between the soil surface and the groundwater table. In this zone, air and water are present in the pores, but the soil is not completely saturated. The Vadose Zone plays an important role in water infiltration, gas exchange, and nutrient exchange for plants. As shown in Figure 2, the Vadose zone consists of surface soils, unsaturated subsurface material, and the capillary fringe zone. The subsurface material consists of partially weathered soils and unweathered parent material. The Vadose zone can be very shallow (less than 1 m) or very deep (extending hundreds of meters or more), depending on the depth of the groundwater table [30].

Currently, there are stability analysis methods, including the Limited Equilibrium Method (LEM), Finite Element Method (FEM), and Finite Difference Method (FDM). Among the above methods, LEM is more commonly used than other methods.

The Factor of Safety (FoS) according to the LEM is determined through considering the moment equilibrium and/or force equilibrium (vertical and/or horizontal). Depending on the approach, the limit equilibrium method is divided into the following methods: Fellenius, Ordinary, Bishop simplified, Jambu corrected, Morgenstern-Price, and Spencer (Table 1). The sliding body is divided into several sections (soil columns), and the stability of each section is analyzed (considering the normal and tangential forces on both sides of the soil column). Then, all the sections are combined to calculate the factor of safety for the assumed sliding surface. To obtain the smallest safety factor (corresponding to the most dangerous sliding surface) of the slope, several assumed sliding surfaces are

analyzed to determine the smallest stability factor. The method is suitable for both homogeneous and heterogeneous slopes, complex stratigraphic conditions, and considers non-uniform pore water pressures, a variety of linear and nonlinear shear strength models, along with almost any sliding surface geometry, loads (distributed and concentrated), earthquakes, structural reinforcement (anchors, geotextiles, roots), and cracks on slopes.

Table 1. Sliding surfaces and equilibrium forms of the methods in the Limit Equilibrium Method [31]

| Method | Sliding surface | | Equilibrium | |
|-------------------|-----------------|--------------|-------------|-------------------------|
| | Circular | Non-Circular | Moment | Force |
| Fellenius | yes | no | yes | no |
| Ordinary | yes | no | yes | no |
| Bishop simplified | yes | no | yes | vertical |
| Jambu simplified | yes | yes | yes | vertical and horizontal |
| Morgenstern-Price | yes | yes | yes | vertical and horizontal |
| Spencer | yes | yes | yes | vertical and horizontal |

In this paper, the Seep/W and Slope/W modules in the GeoStudio software were applied for simulation. The combination of these two modules brought a comprehensive analysis, which mainly included the following two steps: (1) the FEM of the Seep/W module was used to analyze the unsteady seepage caused by rain and other climatic factors such as temperature, humidity, evaporation, wind velocity, especially considering the characteristics of vegetation cover on the slope; (2) The unsteady seepage results from the Seep/W module will be imported into the Slope/W module to analyze and determine the factor of safety by the LEM. Specifically, the total LEM of Morgenstern-Price has been selected; the stability factor satisfies both the force balance (vertical and horizontal) and the moment balance (Figure 3).

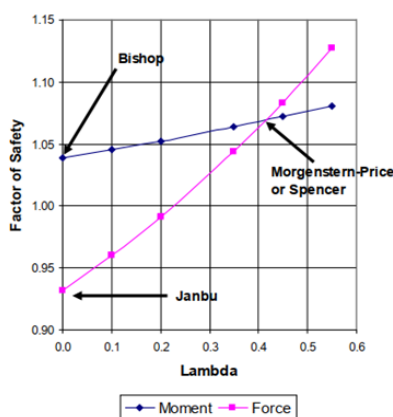


Figure 3. Factor of safety according to the Bishop, Janbu, and Morgenstern-Price or Spencer methods [31]

3. Dak Pring Case Study

3.1. Study Area

Dak Pring Hydropower Plant is located in Cha Val Commune, Nam Giang District, Quang Nam Province, approximately 40 km west of Thanh My Town, Nam Giang

District, and 160 km northwest of Tam Ky City, with coordinates 15°38'19,46" N; 107°33'14,69" E. The project began in April 2015 and was completed on 30 May 2017, with the main task of generating electricity. It has a capacity of 7,5MW (02 units) and an average annual electricity output of 30,47 million kWh.



Figure 4. Landslide location seen from the yard of Dak Pring Hydropower Plant (November 2017)

After heavy rainfall event from 4 November 2017 to 6 November 2017, the natural hillside upstream of Dak Pring Hydropower Plant experienced two landslides, each about 10m wide, 20m long, and 6m deep. The material in these two slides moved down about 5m -10m into the plant's yard and remained partly on the slope upstream of the plant (Figure 4).

3.2. Geological conditions

Table 2. Physical and mechanical indicators of soil and rock layers [32]

| Layer | γ_w | ϕ | C | E | ν | K (m/s) |
|-----------------|----------------------|----------|-----|-----------------------|-------|----------------------|
| | (kN/m ³) | (degree) | kPa | (kg/cm ²) | | |
| edQ | 18 | 19 | 27 | 90 | 0.20 | 5×10^{-7} |
| IA ₁ | 19 | 21 | 24 | 150 | 0.25 | 1×10^{-6} |
| IA ₂ | 25.4 | 26.6 | 50 | 3,000 | 0.40 | 5.8×10^{-6} |
| IB | 27.0 | 33 | 200 | 20,000 | 0.30 | 1.2×10^{-5} |
| IIA | 28.2 | 40.4 | 350 | 70,000 | 0.25 | 3.5×10^{-6} |
| IIB | 28.4 | 42 | 450 | 100,000 | 0.20 | 5.8×10^{-7} |

γ_w - Unit Weight; ϕ - Internal Friction Angle; C - Soil Cohesion; E - Elastic Modulus; ν - Poisson Ratio; K - Coefficient of Permeability.

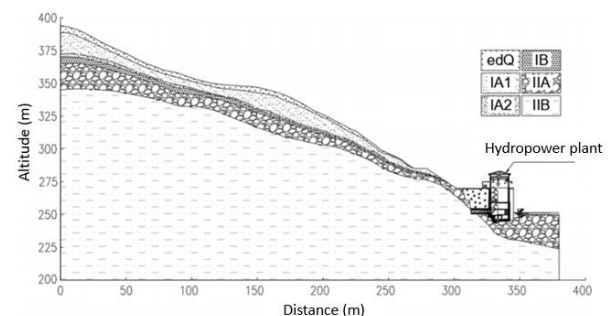


Figure 5. Topographical and geological conditions of Dak Pring project

The typical cross-section is selected at the factory location, where the landslide occurred with borehole DP22, including 06 stratigraphic layers: the remnant slope layer and the strongly weathered rock zone (edQ + IA₁) with a thickness of 7-10m, which is prone to landslides; the strongly weathered rock zone (IA₂) with a thickness of 1-2m; the IB rock zone is 0-2m thick, below is the IIA rock zone belonging to the Ben

Giang - Que Son complex, hard and solid rock; and the IIB rock zone is hard and very hard rock (Figure 5). The groundwater level at the foot of the slope is 2-5m below the ground, higher than the bottom of the factory foundation and the channel [32]. Physical and mechanical properties of soil and rock layers are provided in Table 2.

3.3. Climate conditions

Dak Pring Hydropower Plant is located on the eastern slope of the Truong Son Mountain and to the west of Quang Nam province, so it has a tropical monsoon climate. The west has a different rainfall regime and hydrological characteristics from the deltas to the sea in the east. The average annual air temperature varies between 20°C ÷ 28°C, the lowest temperature is 8.7°C, and the absolute maximum temperature reaches 41°C. The average monthly relative humidity in the area is quite stable; during the rainy season it varies from 80% ÷ 90%. During the year, there is a lot of sunshine from April to August; the number of hours of sunshine in these months is usually over 200 hours; the most sunshine is in May and June; the average number of hours of sunshine is up to approximately 250 hours/month. There is little sunshine from September to March, in which the month with the least sunshine is December (less than 100 hours). During the year, there are 2 wind seasons: the summer monsoon from May to September, with prevailing winds from the west and southwest at an average speed of 1.46 m/s, and the winter monsoon from November to April with prevailing winds from the southwest at an average speed of 1.47 m/s. Annual rainfall is quite large but unevenly distributed throughout the year. The rainy season, from September to December, accounts for 60% ÷ 75% of the total annual rainfall, while the dry season lasts from January to August. In May and June, secondary rainfall peaks appear, becoming more pronounced further west in the study area and creating a sub-seasonal period in the basin. The period of heaviest rainfall in the whole region is often concentrated in October and November [33].

The climatic conditions for the analysis of unsteady seepage flow were taken from actual data measured from 25 October 2017 to 16 November 2017, including temperature, humidity, wind speed, and rainfall. Rainfall data was observed at Hien station (Dong Giang) from 25 October 2017 to 16 November 2017, representing a typical rainfall model in the study area. Other meteorological data was taken from Tam Ky meteorological station. The meteorological data series used in the model during the calculation period from 25 October 2017 to 16 November 2017 is shown in Figures 6 to 9.

In addition, according to Decision 18/2021/QĐ-TTg 22 April 2021 of the Prime Minister on "Regulations on projects, warnings, transmission of natural disasters and levels of natural disaster risks", the authors conducted slope stability calculations for four rainfall scenarios according to four levels of natural disaster risks (RRTT) (level I, level II, level III and level IV) due to heavy rain in the mountainous area of Quang Nam province, as prescribed in Table 3. The rainfall model for the four risk levels is scaled from the typical rainfall model (Figure 9), and the cumulative rainfall chart is shown in Figure 10.

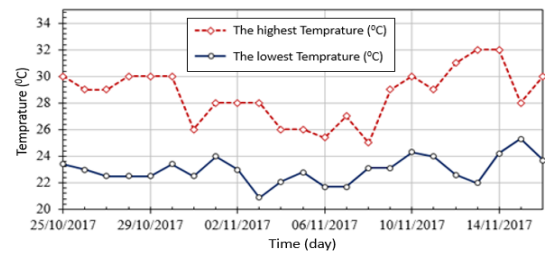


Figure 6. Temperature graph

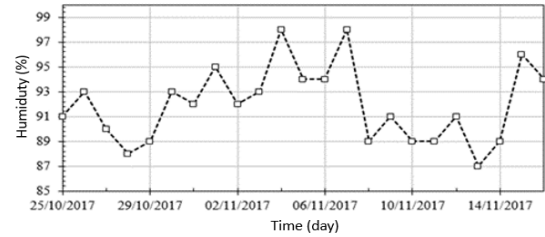


Figure 7. Humidity graph

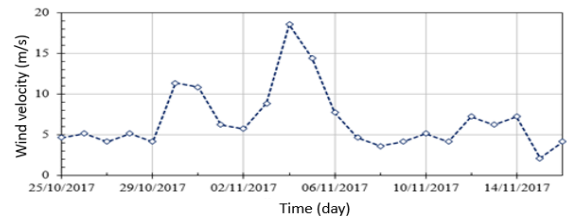


Figure 8. Wind velocity graph

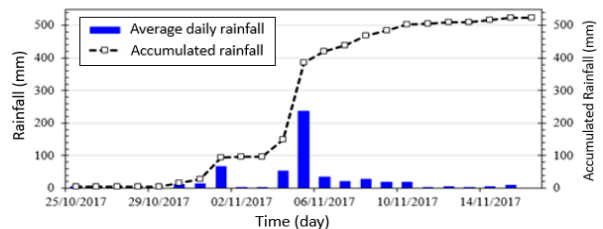


Figure 9. Daily rainfall graph

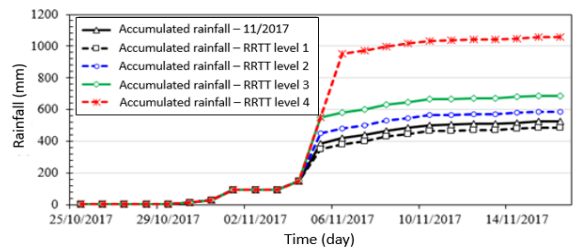


Figure 10. Cumulative rainfall of typical rainfall model (November 2017) and 4 levels of RRTT

Table 3. Maximum rainfall of scenarios

| November 2017 | RRTT Level I | RRTT Level II | RRTT Level III | RRTT Level IV |
|--|------------------------|------------------------|----------------------|----------------------|
| 235,8 mm (05 November) | (100-200) mm/ 24 hours | (200-400) mm/ 24 hours | Over 400mm/ 24 hours | Over 400mm/ 48 hours |
| Maximum daily rainfall used for scaling for RRTT levels (mm/ 24 hours or 48 hours) | | | | |
| 235,8 (05/11/17) | 200 | 300 | 400 | 400 |

RRTT: Natural disaster risk.

Source: Decision 18/2021/QĐ-TTg dated April 22, 2021 of the Prime Minister on "Regulations on forecasting, warning, transmitting information about natural disasters and levels of natural disaster risk".

3.4. Vegetation conditions

The data needed to consider the influence of land cover conditions in the seepage and stability analysis include Leaf Area Index (LAI) and Root Depth. The study area is in the Western Truong Son Mountain range, a low mountainous area, with a natural elevation of 400 m to 700 m, slope varying from 20° to 45°, and dense vegetation including climbing plants and tropical woody plants. Refer to the research results on LAI [34] and Root Depth [35]. For mature tropical woody plants, the cover system conditions were determined to be 2.0 and 0.4 m, respectively.

4. Results and Discussion

In this study, the factors assigned to the seepage problem (rainfall, temperature, humidity, and wind) are time series data. Therefore, the results of the seepage analysis according to the unsteady seepage, meaning that the results of determining the infiltration flow characteristics change depending on the time of extraction of the results.

For the November 2017 rainfall event scenario using the observation timeseries data from 25 October 2017 to 15 November 2017, the authors defined the calculation period as 24 hours (1 day and night) with 22 steps. The slope stability calculation for the November 2017 scenario uses the Slope/W module connected to the Seep/W module to analyze the seepage flow due to rain, while taking into account the climatic conditions (temperature, humidity, and wind speed) and vegetation cover (Leaf Area Index and Root Depth) as outlined in Section 3.4. The FoS results at step #15, as of 8 November 2017, are shown in Figure 11c. The results of the model show that there are 6 calculation steps (#14 ÷ #19) with FoS less than 1, which proves that the rainfall event in November 2017 will cause the landslide of the Dak Pring hydropower plant. This result is consistent with the fact that the slide has occurred. In addition, the location of the slide that occurred was located on the simulated cross-section (Figure 11a) consistent with the simulation results in Figure 11b. This shows that the slope stability simulation model has high reliability.

The authors also calculated the stability of the rainfall process corresponding to 4 levels of RRTT (according to rainfall intensity) according to Decision 18/2021/QD-TTg. The results of the FoS chain according to 22 calculation steps are listed in Table 4. The results illustrate the smallest FoS for the most dangerous sliding surface for the RRTT levels (levels I to IV) respectively, as shown in Figures 12 to 15.

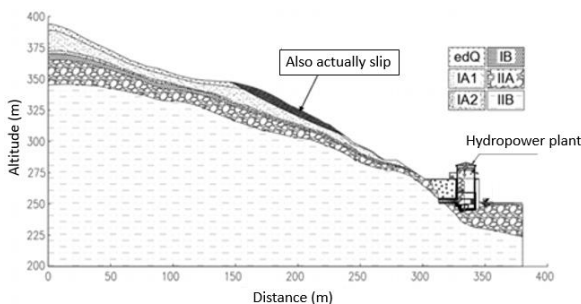


Figure 11a. Actual sliding surface in Dak Pring

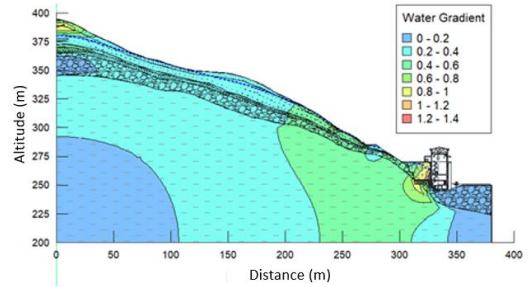


Figure 11b. Seepage calculation results (velocity vector and permeability gradient) of slope at step #15 (8 November 2017)

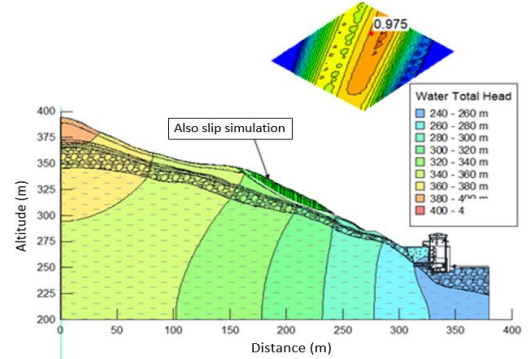


Figure 11c. FoS result at step #15 (8 November 2027)

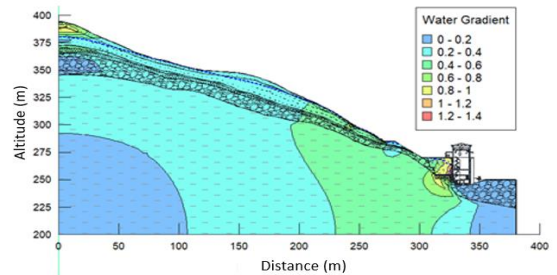


Figure 12a. Seepage calculation results (velocity vector and permeability gradient) of slope with RRTT level I at step #15

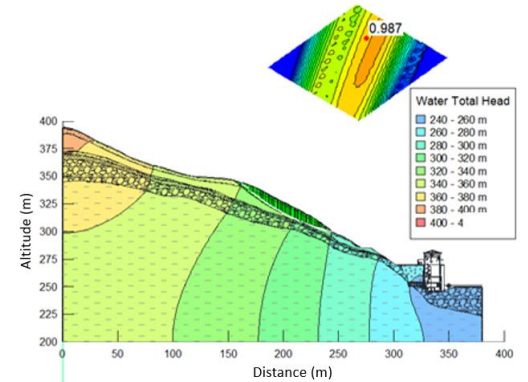


Figure 12b. FoS result with RRTT Level I at step #15

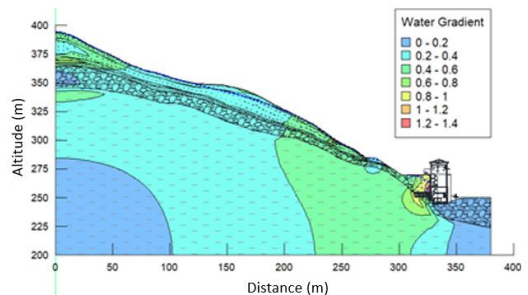


Figure 13a. Seepage calculation results (velocity vector and permeability gradient) of slope with RRTT level II at step #15

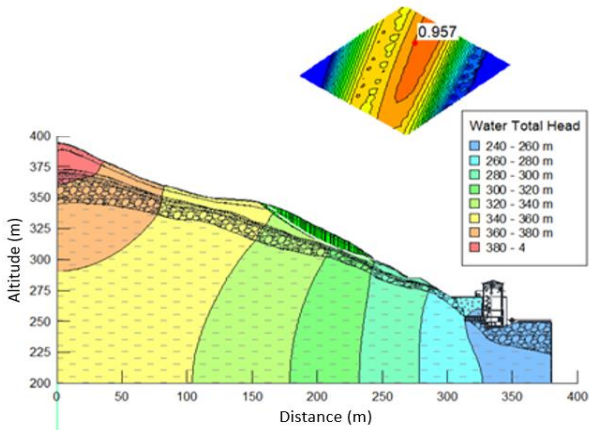


Figure 13b. FoS result with RRTT Level II at step #15

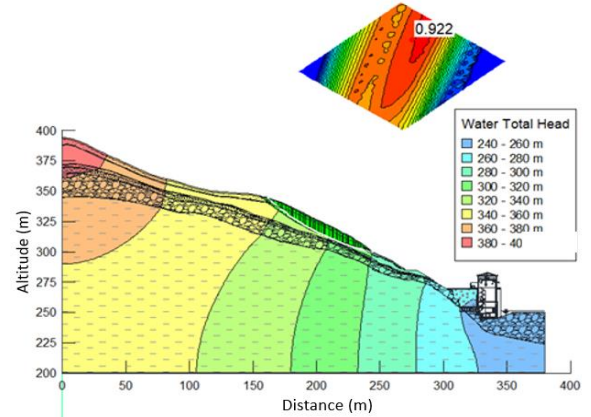


Figure 15b. FoS result with RRTT Level IV at step #15

Table 4. Summary FoS results (22 calculation steps) according to scenarios

| Time #Timestep | Factor of Safety | | | | |
|----------------|------------------|--------------|---------------|----------------|---------------|
| | November 2017 | RRTT Level I | RRTT Level II | RRTT Level III | RRTT Level IV |
| 25/10/2017 #01 | 1,078 | 1,078 | 1,078 | 1,078 | 1,078 |
| 26/10/2017 #02 | 1,077 | 1,077 | 1,077 | 1,077 | 1,077 |
| 27/10/2017 #03 | 1,078 | 1,078 | 1,078 | 1,078 | 1,078 |
| 28/10/2017 #04 | 1,078 | 1,078 | 1,078 | 1,078 | 1,078 |
| 29/10/2017 #05 | 1,078 | 1,078 | 1,078 | 1,078 | 1,078 |
| 30/10/2017 #06 | 1,078 | 1,078 | 1,078 | 1,078 | 1,078 |
| 31/10/2017 #07 | 1,078 | 1,078 | 1,078 | 1,078 | 1,078 |
| 01/11/2017 #08 | 1,077 | 1,077 | 1,077 | 1,077 | 1,077 |
| 02/11/2017 #09 | 1,075 | 1,075 | 1,075 | 1,075 | 1,075 |
| 03/11/2017 #10 | 1,049 | 1,049 | 1,049 | 1,049 | 1,049 |
| 04/11/2017 #11 | 1,065 | 1,065 | 1,065 | 1,065 | 1,065 |
| 05/11/2017 #12 | 1,075 | 1,075 | 1,075 | 1,075 | 1,075 |
| 06/11/2017 #13 | 1,049 | 1,049 | 1,049 | 1,049 | 1,049 |
| 07/11/2017 #14 | 0,992 | 1,000 | 0,972 | 0,951 | 0,951 |
| 08/11/2017 #15 | 0,975 | 0,987 | 0,957 | 0,952 | 0,922 |
| 09/11/2017 #16 | 0,978 | 0,988 | 0,969 | 0,966 | 0,960 |
| 10/11/2017 #17 | 0,980 | 0,991 | 0,973 | 0,972 | 0,967 |
| 11/11/2017 #18 | 0,988 | 0,994 | 0,982 | 0,981 | 0,977 |
| 12/11/2017 #19 | 0,995 | 0,999 | 0,989 | 0,988 | 0,985 |
| 13/11/2017 #20 | 1,013 | 1,017 | 1,008 | 1,007 | 1,004 |
| 14/11/2017 #21 | 1,022 | 1,025 | 1,018 | 1,017 | 1,014 |
| 15/11/2017 #22 | 1,035 | 1,039 | 1,032 | 1,031 | 1,029 |

The results in Table 4 and Figure 16 show that, under normal climatic conditions (temperature, humidity, and wind speed as in Figures 6, 7 and 8 respectively) without rain, the FoS is 1.078. Therefore, the natural slope ensures stability under no rain conditions.

In the first rainy day, the stability coefficient of the slope does not decrease immediately at the time of rain; it has a delay depending on the intensity of the rain as well as the continuity of the rain. Similarly, when there is a rain break, the stability coefficient also has a delay for the stability coefficient to recover. Specifically, the phase shift of FoS over time compared to the rainfall intensity chart is 1 day for light rainfall intensity (< 5 mm/day); 2 days for rainfall intensity of about (10 ÷ 20) mm/day; and (3 ÷ 4) days for rainfall intensity of about > 100 mm/day. In addition, the

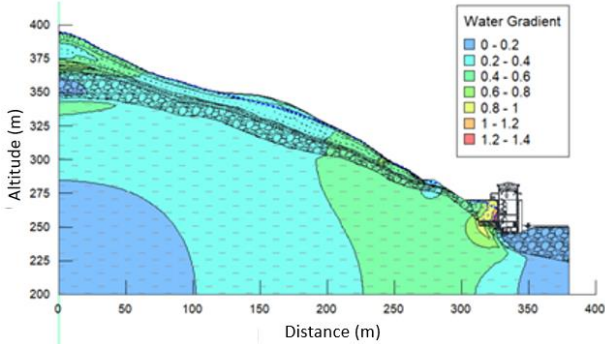


Figure 14a. Seepage calculation results (velocity vector and permeability gradient) of slope with RRTT level III at step #14

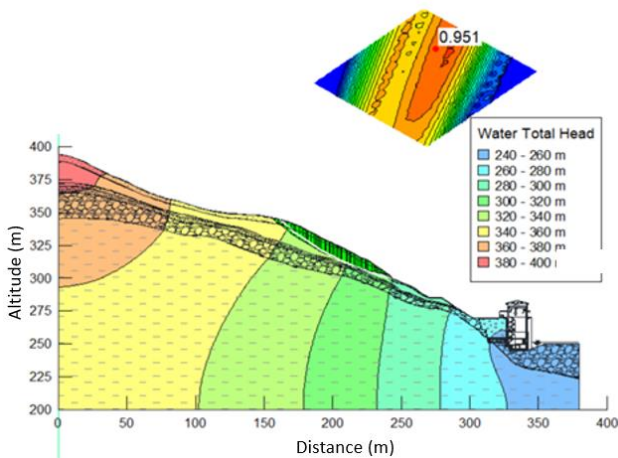


Figure 14b. FoS result with RRTT Level III at step #14

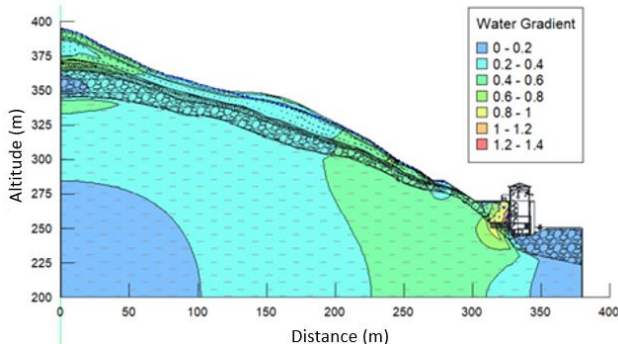


Figure 15a. Seepage calculation results (velocity vector and permeability gradient) of slope with RRTT level IV at step #15

phase shift is also significantly affected by the cumulative effect of the continuity of rainfall event, and it is not easy to accurately determine the value of this phase shift.

In 5 scenarios, including the actual rainfall model in November 2017 and 4 scenarios for 4 levels of RRTT with the rainfall model scaled from the typical rainfall model. The results show that: In RRTT level I, the Dak Pring slope will lose stability on the 15th to the 19th day (calculation step #15 to #); RRTT from level II to level IV, the time of landslide is 1 day earlier, from the 14th to the 19th day; especially for the RRTT level III (with 1 day of rain 400 mm/day in the rainfall model) with the smallest FoS is 0.951, while the level IV RRTT (with 2 consecutive days of rain 400 mm/day in the rainfall model) has the smallest FoS is 0.922, which means that the daily rainfall intensity remains unchanged but the prolonged rainfall will increase the risk of slope landslide.

Landslides occur when the shear stress caused by the sliding body exceeds the shear strength of the material. For landslides caused by rainfall, water seeps into the ground, increasing the pore water pressure in the landslide body, thereby reducing the effective normal stress ($\sigma - p$). The higher the level of seepage flow caused by rain into the slope, the more reduction in effective normal stress, leading to an increased risk of slope instability. On the contrary, with low-intensity rains, the affected area and/or the level of influence of the reduction in effective normal stress is insignificant or not large enough to cause the slope to collapse.

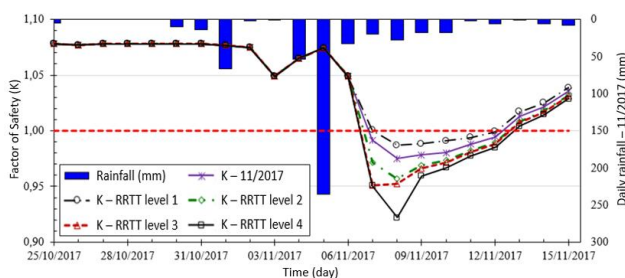


Figure 16. Graph of FoS of scenarios

5. Conclusion

The article has studied the seepage - slope stability model with a comprehensive and detailed approach, considering the impact of changes in rainfall and the characteristics of vegetation and roots. Some conclusions are summarized as follows:

- Landslides are influenced by various factors, with seepage due to rain being the most common cause, especially in tropical regions. In tropical regions, rain often lasts for extended periods, and in mountainous areas, the soil layer covering the bedrock has a relatively large water absorption. Therefore, stability calculations need to apply the theory of unsaturated soil mechanics for analysis, as this approach will yield results that are more consistent with reality.

- There is a phase shift of FoS compared to the graph of rainfall intensity over time. In the November 2017 rainfall event, high-risk instability often appeared 1 to 2 days after

periods of heavy rainfall. Indeed, the slope instability ($FoS < 1.0$) did not occur during the peak rainfall on 5 November; instead, the FoS decreased from 1.075 to 1.049 on 6 November and further decreased to 0.992 on 7 November. This comes from the infiltration process and the effect of vegetation layers, root systems, and water saturation in the Vadose area as analyzed.

- For the rainfall scenarios according to RRTT levels from I to IV, the trend of decreasing and recovering the stability coefficient is similar to the rain in November 2017. The FoS decreases as the rainfall intensity increases, with the corresponding minimum FoS values for RRTT levels I, II, III, and IV being 0.987, 0.957, 0.951, and 0.922, respectively.

- The slope stability coefficient does not decrease immediately when it rains; rather, there is a delay in the decrease of the stability coefficient, which depends on the rainfall intensity, continuity, and the cumulative rainfall. However, determining the exact value of this phase shift is challenging, indicating a need for further research on this topic.

REFERENCES

- [1] B. T. Dilley, "Vulnerability of the Venezuelan Population to Natural Disasters", *Environmental Hazards*, vol. 3. No. 3, pp. 167-182, 2001.
- [2] K. M. Gündoğan, "Assessment of Landslide Risk in Turkey", *Natural Hazards*, vol. 3, no. 3, pp. 337-354, 2004.
- [3] R. K. S. Sharma, "Landslide Disaster in Uttarakhand: A Study of the 2013 Event", *Journal of Environmental Management*, vol. 146, pp. 1-9, 2014.
- [4] W. K. Wozniak, "The Oso Landslide: A Case Study of Landslide Risk and Response", *Landslides*, vol. 12, no. 5, pp. 1015-1024, 2015.
- [5] M. Ghimire, "Assessment of Landslide Risk in Nepal Following the 2015 Earthquake", *Geosciences*, vol. 6, no. 3, pp. 28-36, 2016.
- [6] Z. Z. Xu, "Landslides Triggered by the 2017 Sichuan Earthquake", *International Journal of Disaster Risk Reduction*, vol. 28, pp. 202-210, 2018.
- [7] D. Petley, "Global patterns of loss of life from landslides", *Geology*, vol. 40, no. 2, pp. 107-110, 2012. DOI: 10.1130/G32490.1.
- [8] T. Q. H. Nguyen, "Assessing the damage caused by landslides in Vietnam", *Journal of Geographical Sciences*, vol. 24, no. 3, pp. 112-120, 2016.
- [9] P. e. a. Gautam, "Landslide susceptibility mapping with GIS in high mountain area of Nepal: a comparison of four methods", *Environmental Earth Sciences*, vol. 80, no.9, pp. 359-366, 2021.
- [10] P. Ram and V. Gupta, "Landslide hazard, vulnerability, and risk assessment (HVRA), Mussoorie township, lesser himalaya, India", *Environment, Development and Sustainability*, vol. 24, pp. 473-501, 2022.
- [11] A. Zamroni, A. C. Kurniati, and H. N. E. Prasetya, "The assessment of landslides disaster mitigation in Java Island, Indonesia: a review", *Journal of Geoscience, Engineering, Environment, and Technology*, vol. 5, no. 3, pp. 124-128, 2020.
- [12] D. Wang, M. Hao, S. Chen, Z. Meng, D. Jiang, and F. Ding, "Assessment of landslide susceptibility and risk factors in China", *Natural hazards*, vol. 108, pp. 3045-3059, 2021.
- [13] N. D. Ha and N. H. Duong, "Advancements, Challenges, and Future Directions in Rainfall-Induced Landslide Prediction: A Comprehensive Review", *Journal of Engineering & Technological Sciences*, Vol. 55, no. 4, pp. 466-478, 2023.
- [14] T. T. T. Le and S. Kawagoe, "Impact of the landslide for a Relationship between Rainfall Condition and Land Cover in North Vietnam", *J. Geol. Resour. Eng.*, vol. 6, pp. 239-250, 2018.

- [15] D. H. Loi, L.H. Quang, K. Sassa, K. Takara, K. Dang, N. K. Thanh, and P. V. Tie., "The 28 July 2015 rapid landslide at Ha Long City, Quang Ninh, Vietnam", *Landslides*, vol. 14, pp. 1207-1215, 2017.
- [16] H. T. Nguyen, "Landslide risk analysis in Hoa Binh", *Journal of Geology and Minerals*, vol. 34, no. 2, pp. 112-120, 2018.
- [17] Q. H. Le, "Impact of heavy rain on landslides in Son La", *Journal of Geographical Sciences*, vol. 25, no. 1, pp. 78-85, 2019.
- [18] T. T. Phan, "Assessing damage caused by landslides in Nghe An", *Environmental Protection*, vol. 22, no. 4, pp. 34-39, 2021.
- [19] T. A. Tuan, P. D. Pha, T.T. Tam, and D. T. Bui "A new approach based on Balancing Composite Motion Optimization and Deep Neural Networks for spatial prediction of landslides at tropical cyclone areas", *IEEE Access*, vol. 11, pp. 69495-69511, 2023.
- [20] G. Wang and K. Sassa, "Pore-pressure generation and movement of rainfall-induced landslides: effects of grain size and fine-particle content", *Eng Geol*, vol. 69, no. 1-2, pp. 109-125, 2003.
- [21] M. Lora, M. Camporese, P. A. Troch, and P. Salandin, "Rainfall-triggered shallow landslides: infiltration dynamics in a physical hillslope model", *Hydrol Process*, vol. 30, no. 18, pp. 3239-3251, 2016.
- [22] K. Sasahara, "Prediction of the shear deformation of a sandy model slope generated by rainfall based on the monitoring of the shear strain and the pore pressure in the slope", *Eng Geol*, vol. 224, pp. 75-86, 2017.
- [23] S. Zhang, X. Zhang, X. Pei, S. Wang, R. Huang, Q. Xu, and Z. Wang, "Model test study on the hydrological mechanisms and early warning thresholds for loess fill slope failure induced by rainfall", *Eng Geol*, vol. 258, pp. 105-135, 2019.
- [24] D. Bhattacharjee and B. V. S. Viswanadham, "Effect of geocomposite layers on slope stability under rainfall condition", *Indian Geotech J*, vol. 48, no. 2, pp. 316-326, 2018.
- [25] A. C. Trandafir, R. C. Sidle, T. Gomi, and T. Kamai, "Monitored and simulated variations in matric suction during rainfall in a residual soil slope", *Environ Geol*, vol. 55, no. 5, pp. 951-961, 2008.
- [26] A. K. Leung, and NG. C. W. Wai, "Analyses of groundwater flow and plant evapotranspiration in a vegetated soil slope", *Can Geotech J.*, vol. 50, no. 12, pp. 1204-1218, 2013.
- [27] S. Bandara, A. Ferrari, and L. Laloui, "Modelling landslides in unsaturated slopes subjected to rainfall infiltration using material point method", *Int J Numer Anal Met*, vol. 40, no. 9, pp. 1358-1380, 2016.
- [28] Y. Tang, W. Wu, K. Yin, S. Wang, and G. Lei, "A hydro-mechanical coupled analysis of rainfall induced landslide using a hypoplastic constitutive model", *Comput Geotech*, vol. 112, pp. 284-292, 2019.
- [29] E. T. Mohsen and A. A. Behzad, "A Modeling Platform for Landslide Stability: A Hydrological Approach", *Water*, vol. 11, pp. 2146, 2019.
- [30] J. Ren, *Interpretation of the frozen soils behavior extending the mechanics of unsaturated soils*, in Doctoral dissertation, Université d'Ottawa/University of Ottawa, 2019.
- [31] G. I. Ltd, *Stability Modeling with GeoStudio*, Geoslope, 2024.
- [32] Power engineering consulting joint stock company 1, *Survey records of topography, geology, hydrometeorology of Dak Pring Hydropower Plant*, 2012.
- [33] T. Tuyen, *Hydro-Climatic Characteristics of Quang Nam Province (1980-2020)*, Quang Nam hydrometeorological Station, 2023.
- [34] Y. Tanioka, Y. Cai, H. Ida, and M. Hirota, "A spatial relationship between canopy and understory leaf area index in an old-growth cool-temperate deciduous forest", *Forests*, Vol. 11, pp. 1-11, 2020.
- [35] F. L. Li and W. K. Bao, "New insights into leaf and fine-root trait relationships: Implications of resource acquisition among 23 xerophytic woody species", *Ecology and Evolution*, Vol. 5, no.22, pp. 5344-5351, 2015.